A Study on Delocalization of MLCT Excited States by Rigid Bridging Ligands in Homometallic Dinuclear Complexes of Ruthenium(II)

Leif Hammarström,*,†,‡ Francesco Barigelletti,*,† Lucia Flamigni,† Maria Teresa Indelli,§ Nicola Armaroli,† Giuseppe Calogero,† Massimo Guardigli,† Angelique Sour,|| Jean-Paul Collin,*,|| and Jean-Pierre Sauvage*,||

Istituto FRAE-CNR, Via Gobetti 101, I-40129 Bologna, Italy, Department of Physical Chemistry, University of Uppsala, Box 532, S-75121 Uppsala, Sweden, Centro di Fotoreattività e Catalisi CNR, Dipartimento di Chimica, Università di Ferrara, via L. Borsari 46, I-44100 Ferrara, Italy, and Laboratoire de Chimie Organo-Minerale, Université Louis Pasteur, Faculté de Chemie, 4 rue Blaise Pascal, F-67008 Strasbourg, France

Received: June 9, 1997; In Final Form: September 4, 1997[⊗]

For the structurally rigid homometallic dinuclear complexes (ttp)Ru(tpy-tpy)Ru(ttp)$^{4+}$ and (ttp)Ru(tpy-ph-tpy)Ru(ttp)$^{4+}$, we have obtained ground-state absorption spectra and transient-absorption difference spectra at room temperature and luminescence spectra and lifetimes in the temperature interval from room temperature to the rigid matrix (90 K); the solvent was acetonitrile or butyronitrile (tpy is 2,2′:6′,2″-terpyridine, ttp is 4′-*p*-tolyl-2,2′:6′,2″-tpy, and ph is 1,4-phenylene). The gathered spectroscopic data indicate that after absorption of visible light, formation of the luminescent metal-to-ligand charge transfer (MLCT) excited states takes place, which involves the bridging ligand (BL). Since we found that (ttp)Ru(tpy-tpy)Ru(ttp)$^{4+}$ is a good luminophore (λ_{max} = 720 nm, $\Phi = 4.7 \times 10^{-3}$, and τ = 570 ns) while both (ttp)Ru(tpy-ph-tpy)Ru(ttp)$^{4+}$ (λ_{max} = 656 nm, $\Phi = 1.1 \times 10^{-4}$, and τ = 4 ns) and the reference mononuclear complex Ru(ttp)$_2^{2+}$ (λ_{max} = 640 nm, $\Phi = 3.2 \times 10^{-5}$, and τ = 0.9 ns) are not, we have explored the effects brought about by the delocalization and energy content of the luminescent state. The study of the temperature dependence of the luminescence lifetimes indicates that two main nonradiative paths, i and ii, are responsible for deactivation of the luminescent state. Path i directly connects the luminescent and ground states; within the frame of the "energy-gap law", vibronic analysis of low-temperature luminescence profiles enables one to correlate the delocalization of the M → BL CT state and the extent of structural distortions occurring at the accepting ligand. Thermally activated decay via a metal-centered (MC, of dd orbital origin) excited state characterizes path ii, with a MLCT−MC energy separation ΔE = 3800, 2300, and 1600 cm^{-1} for (ttp)Ru(tpy-tpy)Ru(ttp)$^{4+}$, (ttp)Ru(tpy-ph-tpy)Ru(ttp)$^{4+}$, and Ru(ttp)$_2^{2+}$, respectively. At room temperature, for this limited series of complexes it is found that nonradiative processes governed by the "energy-gap law" play a minor role as compared to thermally activated processes, the ratios of the rate constants being $k_{nr}^{act}/k_{nr}^{dir} \approx$ 16, 1900, and 7000 for (ttp)Ru(tpy-tpy)Ru(ttp)$^{4+}$, (ttp)Ru(tpy-ph-tpy)Ru(ttp)$^{4+}$, and Ru(ttp)$_2^{2+}$, respectively.

Introduction

The assembly of molecular components via covalent bonds greatly enhances the possibilities to control the intercomponent processes and the function of multicomponent systems because the reactants can be fixed at a well-defined distance and (sometimes) orientation.[1] This approach has been very helpful for the advancement in the field of photoinduced electron and energy transfer (PET and PEnT).[2] The extension to multicomponent supermolecules has been accompanied by an increasing ablility to control the PET and PEnT reactions and obtain sophisticated functions, such as stabilization of photoinduced charge separation,[3] multielectron collection,[4] harvesting of excitation energy in artificial antennas,[5] and various logical and switching functions.[6]

Transition-metal complexes of Ru(II), Os(II), Re(I), Rh(III), and Ir(III) feature favorable electrochemical, photophysical, and photochemical properties.[7,8] Therefore, such complexes have been extensively used to construct polynuclear species, due to the relative ease of using a modular synthetic approach in coordination compounds.[8] However, as the number of components increases, there is an increasing difficulty to maintain a well-defined structure of the resulting supermolecule. For instance, complexes obtained from bidentate bpy-type ligands with Ru(II), including the most widely used Ru(bpy)$_3^{2+}$, are chiral (bpy is 2,2′-bipyridine); furthermore, with a single substituent on each ligand, the bidentate ligand is generally not symmetric, giving four isomers for each homoleptic complex (*cis/trans* and *fac/mer*).[9] Thus, the use of tris(bidentate) coordination to fill the octahedral environment around the Ru(II) center for building up polynuclear assemblies may result in a large number of isomers.

From a geometrical viewpoint, a convenient building block for the construction of multicomponent species is the Ru(tpy)$_2^{2+}$ unit (tpy is 2,2′:6′,2″-terpyridine).[10] This is because Ru(tpy)$_2^{2+}$ is nonchiral, and if X and Y substituents are introduced in the para position of the central ring of each terpyridine,[11] there are still no isomers, Chart 1. In this way, rodlike polynuclear molecules can be constructed where each component unit is lying on a well-defined molecular axes, the long axis of the molecular rod.[12,13] The possibility to construct extended, rigid and rodlike supermolecules incorporating electroactive and photoactive units is appealing and may prove advantageous for

† Istituto FRAE-CNR.
‡ University of Uppsala.
§ Università di Ferrara.
|| Université Louis Pasteur.
⊗ Abstract published in *Advance ACS Abstracts,* October 15, 1997.

S1089-5639(97)01875-6 CCC: $14.00

CHART 1

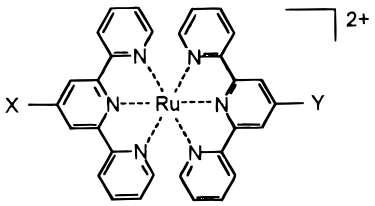

$Ru(tpy)_2^{2+}$ with X and Y substituents

the design of functional supermolecules[6−8,14] for, e.g., signal processing, solar energy conversion, or molecular electronics.

A disadvantage connected with the use of tpy-type complexes of Ru(II) as photoactive units is the short excited-state lifetime (τ) and very low quantum yield (Φ) of emission at room temperature; for the prototypical $Ru(tpy)_2^{2+}$ complex, $\tau = 250$ ps and $\Phi \sim 10^{-5}$.[15] Clearly, these unfavorable properties can severely limit the use of tpy-type Ru(II) complexes as photosensitizers because intrinsic deactivation processes may be much faster than energy or electron transfer to a nearby accepting unit, Chart 1. On this basis, much of the current research is aimed at understanding the role of the various factors that control the photophysical behavior for the family of tpy-type complexes of Ru(II).[10−13] For instance, room-temperature luminescence lifetimes of the order of tens of nanoseconds have been obtained by the introduction of electron-withdrawing or -accepting substituents[11] or by protonation of uncoordinated sites appended to the tpy ligand.[16]

In the present study, we report the photophysical properties of a series of dinuclear Ru(II) complexes with bridging ligands (BL) containing two tpy fragments linked by 0−2 phenylene units, tpy-tpy, tpy-ph-tpy, and tpy-ph_2-tpy, and where the terminal ligand is ttp, Chart 2 (ttp is 4′-*p*-tolyl-2,2′:6′,2″-tpy and ph is 1,4-phenylene). We wished to study the effect of delocalization of the lowest-lying excited states brought about by BL. Recently, this issue has received much attention with regard to the possibility to gain control on (i) the photophysical properties of Ru−polypyridine chromophoric units and, as a consequence, on (ii) the intercomponent processes in multicomponent assemblies incorporating them.[10,12,17] The interest in this study also stems from the possibility to explore intertwined effects connected to electron delocalization[17,18] and the "energy-gap law".[19] Actually, predictions based exclusively on the energy level of the excited states and in agreement with the energy-gap law imply an increase of nonradiative rate constants for decreasing energy levels.[19] However, from the work of Meyer and co-workers,[20] it is known that extended delocalization may lead to a reduction in intrinsic nonradiative processes for chromophores of the Ru(II)−, Os(II)−, and Re(I)− polypyridine type.

In this study we show that delocalization of the luminescent excited state over the bridging ligand of the dinuclear complexes leads to an increase in the emission lifetime at 293 K from ∼1 ns for **Ru** to 570 ns for **Ru-Ru**, with a nearly parallel increase of the luminescence quantum yield. (Schematic formulas for **Ru**, **RuRu**, **Ru-ph-Ru**, and **Ru-ph$_2$-Ru** are illustrated in Chart 2.) A very similar improvement in the luminescence properties has been recently reported for related dinuclear Ru(II) bis(tpy) or tris(bpy) complexes, where the ditopic bridging ligands contained polyene,[17a] ethenyl,[17b,21] or ethynyl[12] spacers. From the photophysical data obtained at 293 and 90 K, from the shape of transient absorption spectra, by measuring the temperature dependence of the emission lifetimes, and from analyses of the luminescence profiles of the low-temperature spectra, we have been able to describe in some detail the underlying changes in the molecular properties responsible for this enhancement of the emission properties. For **Ru-ph$_2$-Ru**, samples at low temperature were cloudy, likely owing to aggregation effects. For this reason, data for this complex are not reported.

CHART 2

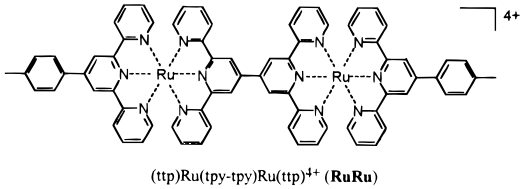

$(ttp)Ru(tpy\text{-}tpy)Ru(ttp)^{4+}$ (**RuRu**)

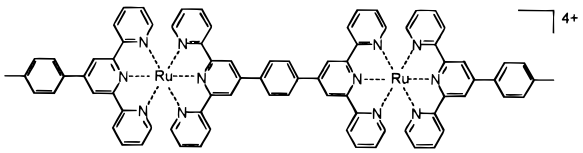

$(ttp)Ru(tpy\text{-}ph\text{-}tpy)Ru(ttp)^{4+}$(**Ru-ph-Ru**)

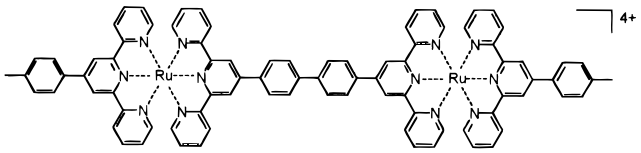

$(ttp)Ru(tpy\text{-}ph_2\text{-}tpy)Ru(ttp)^{4+}$(**Ru-ph$_2$-Ru**)

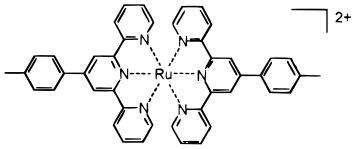

$(ttp)Ru(ttp)^{2+}$(**Ru**)

The chromophore **Ru-Ru** is shown to be an interesting component for the construction of rodlike supermolecules because it is similar to $Ru(bpy)_3^{2+}$ and related complexes containing bidentate ligands in terms of the luminescence properties ($\tau \sim$ hundreds of nanoseconds and $\Phi \sim 10^{-2}$)[7a−c] while conserving the structural advantages of $Ru(tpy)_2^{2+}$ complexes.[10] We show, in particular, that a prominent role in determining the photophysical behavior of the complexes examined is played by the interplay of metal-to-ligand (MLCT) and metal-centered (MC, of dd orbital origin) excited states.[7a−c]

Experimental Section

Synthesis and Characterization. The ligands tpy-tpy, tpy-ph-tpy, and tpy-ph_2-tpy and the dinuclear complexes **Ru-Ru**, **Ru-ph-Ru**, and **Ru-ph$_2$-Ru** have been synthesized and characterized as described previously.[22]

Equipment and Methods. Electrochemical experiments were performed by employing cyclic voltammetry in 0.1 M^{-1} Bu_4NBF_4 on a Pt electrode as described in a previous paper.[23] $E_{1/2}$ values are vs a saturated calomel electrode (SCE). In the dinuclear complexes, the first metal-centered oxidation and ligand-centered reduction processes were found to be two-electron processes, except for reduction of **Ru-Ru**, where two separate waves were observed.[22]

Absorption spectra were recorded with a Perkin-Elmer Lambda 9 spectrophotometer in a dilute (∼10^{-5} M) acetonitrile solution. Luminescence experiments were performed (i) in air-equilibrated or deaerated acetonitrile solutions at room temperature in 1 cm cuvettes, (ii) in a butyronitrile rigid matrix at 77 K (liquid nitrogen temperature) by using samples contained in

capillary tubes immersed in a quartz-finger dewar, and (iii) in butyronitrile solvent in the temperature interval between 293 and 90 K. For the latter case, we employed a Thor Research cryostat and temperature controller. The cryostat was home-modified by substituting the original sample holder with a cell holder for hosting sealed quartz cells. The actual temperature within the cells was obtained through calibration with the help of an external thermocouple, which enabled comparison of the temperatures indicated on the controller with true temperatures monitored by the thermocouple; the uncertainty of the measured temperature was ±2 K. Deaerated samples were prepared at a vacuum line through pump−freeze−thaw repeated cycles and stored in sealed quartz cells.

Luminescence spectra were obtained from a Spex Fluorolog II spectrofluorimeter equipped with a Hamamatsu R928 phototube. Uncorrected luminescence band maxima are used throughout the text unless otherwise stated. To determine the luminescence quantum yields and to analyze the luminescence intensity profiles, we employed corrected luminescence spectra on an energy scale (cm^{-1}). The corrected spectra were obtained either by using a correction curve provided by the firm or by employing a calibrated 45 W quartz−halogen tungsten filament lamp by Optronic Laboratories as a standard for the correction of the phototube response. Luminescence quantum yields Φ_s were computed by following the method described by Demas and Crosby[24] and according to eq 1, where s and r stand for sample and reference standard, respectively, A is the absorbance (taken ≤ 0.1) at the selected excitation wavelength and n is the refractive index of the solvent. $[Ru(bpy)_3]Cl_2$ was chosen as a

$$\frac{\Phi_s}{\Phi_r} = \frac{A_r n_s^2 (\text{area})_s}{A_s n_r^2 (\text{area})_r} \quad (1)$$

reference standard ($\Phi = 2.8 \times 10^{-2}$ in air-equilibrated water[25]). For this complex, it was demostrated that the efficiency of intersystem crossing from the singlet manifold populated by visible light absorption to the formally triplet luminescent state, η_{isc}, is practically unity.[26] For the investigated complexes, we have likewise employed $\eta_{isc} = 1$, as typically assumed for the many members of the Ru-polypyridine family of complexes.[7a−d] The experimental uncertainty in the band maximum for the absorption and luminescence spectra is 2 nm, that for the luminescence quantum yield is 20%. Luminescence lifetimes were obtained with an IBH single-photon-counting apparatus (N_2 lamp, excitation at 337 nm) or with a picosecond fluorescence spectrometer using a Nd:YAG laser (Continuum PY62-10) and a Hamamatsu C1587 streak camera. Both apparatuses have been described previously.[27] The uncertainty on the evaluated lifetimes is 8%.

Transient-absorption spectra on the 30 ps to a few nanosecond time scale were obtained by using a pump and probe apparatus based on the Nd:YAG laser and a double-diode-array detector (Princeton Instruments). Samples were excited at 532 nm (pulse energy ∼ 3 mJ) and probed by a white continuum generated by focusing the 1064 nm fundamental on a D_2O/D_3PO_4 mixture. The time delay between the excitation and probe was adjusted by changing the excitation path via a computer-controlled optical delay stage. The monitoring light, split into two parts, probed irradiated and unirradiated portions of the sample and after the dispersion by a spectrograph, was detected by two diode arrays (sample and reference). Kinetic profiles were constructed by selecting absorbance values, at the desired wavelength, of subsequent time-resolved spectra (typically 20 to 40). Analysis was made by using homemade programs based on standard iterative nonlinear procedures.[28] For time scales larger than 10 ns, nanosecond flash photolysis experiments were performed by using an Applied Photophysics detection system coupled with a Continuum Surelite II Q-switched Nd:YAG laser source. The third harmonic ($\lambda = 355$ nm, half-width of 8 ns, maximum pulse energy of 150 mJ) was used for excitation. The transient signals were recorded on a Lecroy 9360 digital storage oscilloscope and analyzed with routine software.

The vibronic band intensities of the luminescence spectra on an energy scale (cm^{-1}) were analyzed according to a fitting procedure proposed by Meyer and co-workers.[20] For the luminescence spectra obtained at 90 K, one uses a two-mode analysis according to eq 2. where $I(\tilde{\nu})$ is the luminescence

$$I(\tilde{\nu}) = \sum_{\nu_M=0}^{\infty} \sum_{\nu_I=0}^{\infty} \left(\frac{\tilde{\nu}_{00} - \nu_M \tilde{\nu} - \nu_L \tilde{\nu}}{\tilde{\nu}_{00}} \right)^3 \left(\frac{S_M^{\nu_M}}{\nu_M!} \right) \left(\frac{S_L^{\nu_L}}{\nu_M!} \right) \times \exp\left[-(4\ ln\ 2) \left(\frac{\tilde{\nu} - \tilde{\nu}_{00} - \nu_M \tilde{\nu} - \nu_L \tilde{\nu}}{\tilde{\nu}_{1/2}} \right)^2 \right] \quad (2)$$

intensity profile, $\tilde{\nu}_{00}$ is the energy of the 0−0 transition (hereafeter indicated E_{00}), υ are vibrational quantum numbers, M and L are labels for the average and low-frequency modes, S is the displacement parameter along the indicated vibrational mode, and $\tilde{\nu}_{1/2}$ is the bandwith at half-maximum (fwhm) of the vibronic line.

Results

Electrochemistry. Electrochemical potentials have already been reported in conjuction with the intervalence studies of the intermetal interaction for complexes including the **Ru-ph$_n$-Ru** series.[22] It was found that two-electron metal-centered oxidations occurred at +1.31 and +1.27 V vs SCE for **Ru-Ru** and **Ru-ph-Ru**, respectively, to be compared with a metal-centered oxidation of +1.25 V for the reference mononuclear complex **Ru**.[10c,29] Regarding the ligand-centered processes, it was found that reduction steps involving the bridging ligand for the dinuclear complexes occurred at −0.93 (and −1.24), −1.18 (two-electron), and −1.24 V (two-electron) for **Ru-Ru**, **Ru-ph-Ru**, and **Ru**, respectively. Analysis of the intervalence spectra for the Ru(II),Ru(III) species gave values for the intermetal coupling, $H = 0.047$ and 0.030 eV for **Ru-Ru** and **Ru-ph-Ru**, respectively.[22] These results suggest that the intermetal interaction for the dinuclear complexes is not strong, as also inferred by the lack of distinct oxidation waves.[22] Nevertheless, according to widely employed energetic schemes, the second metal center is expected to cause some stabilization of the lowest unoccupied molecular orbital (LUMO) of the bridging ligand and, owing to back-bonding interactions, of the metal-centered highest occupied molecular orbital (HOMO). Because of electrostatic and electronic reasons, this effect is expected (and found) to maximize for **Ru-Ru**. Actually, for this complex two reduction waves were observed, with the first reduction occurring at a more positive potential (by ca. 0.3 V) than that for **Ru**. This provides strong evidence for the first reduction to occur on the tpy-tpy ligand and not on the ttp terminal ligands. On the basis of the known correlation between the electrochemical and spectroscopic properties (absorption and luminescence) concerning the energy position of the MLCT excited states,[7a−c,30] the lowest-lying MLCT states are also expected to reside on the bridging ligands and not on the terminal ligands. A similar line of reasoning concerning BL localization of the lowest MLCT excited state applies for **Ru-ph-Ru** and is in accord with the experimental findings of most dinuclear and polynuclear species.[8,31]

TABLE 1: Spectroscopic and Photophysical Parameters[a]

	absorption		luminescence				
			293 K[b]			90 K[c]	
	λ ($\epsilon \times 10^4$, M^{-1} cm^{-1})		λ_{max}[d] (nm)	τ (ns)	$\Phi \times 10^4$ [e]	λ_{max}[d] (nm)	τ (μs)
Ru-Ru	309 (11.4)	520 (5.8)	720	570 (280)	47	683	12.9
Ru-ph-Ru	308 (12.8)	499 (6.3)	656	4.0 (3.7)	1.1	641	12.3
Ru	306 (7.2)	490 (2.8)	640	0.9	0.32	628	11.0

[a] Acetonitrile solvent unless otherwise specified. [b] Deaerated acetonitrile solvent; in parentheses values for air-equilibrated solvents. [c] Butyronitrile solvent. [d] Band maxima for uncorrected spectra. [e] Quantum yields obtained from corrected spectra and by assuming $\eta_{isc} = 1$, see Experimental Section.

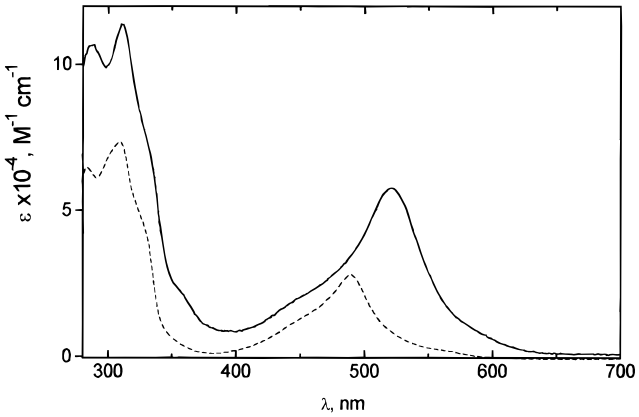

Figure 1. Ground-state absorption spectra for **Ru-Ru** (—) and **Ru** (- - -).

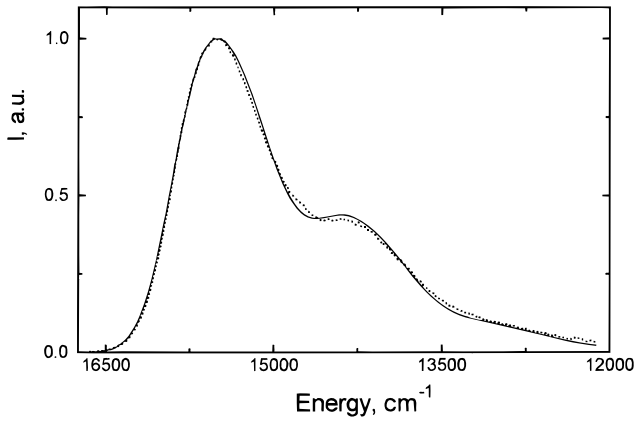

Figure 2. Analysis of the profile of the luminescence spectrum, taken at 90 K, for **Ru-ph-Ru**; the solid line results from the fitting procedure, see text.

TABLE 2: Emission Spectral Fitting Parameters[a]

complex	E_{00} (cm^{-1})	S_M	S_L	fwhm (cm^{-1})
Ru-Ru[b]	14 640	0.35	0.46	840
Ru-ph-Ru[b]	15 700	0.46	0.95	610
Ru[b]	16 000	0.53	0.92	540
$Ru(bpy)_3^{2+}$ [c]	17 200	0.87	0.97	650

[a] From analyses of the profiles of corrected luminescence spectra obtained at 90 K in butyronitrile. [b] Two-mode fitting analysis, eq 2 of text. $\hbar\omega_M = 1300$ cm^{-1} and $\hbar\omega_L = 400$ cm^{-1}, respectively. [c] $\hbar\omega_M = 1350$ cm^{-1}.

Absorption and Luminescence Properties. Table 1 lists the absorption band maxima and intensities, luminescence band maxima, lifetimes, and quantum yields obtained at room temperature and the band maxima and lifetimes observed at 90 K. The intense absorption bands in the UV region ($\epsilon > 10^5$ M^{-1} cm^{-1}) are due to ligand-centered (^{1}LC) transitions, and those occurring in the visible region (490−520 nm) are due to metal-to-ligand (^{1}MLCT) transitions.[7a−d] The absorption spectra exhibited by the dinuclear complexes did not overlap with a doubled spectrum of the component unit, the **Ru** reference complex; for illustration purposes, Figure 1 compares the spectra for **Ru-Ru** and **Ru**. In particular, the MLCT band maxima occurred at longer wavelengths than that for **Ru**, $\lambda_{Ru-Ru} > \lambda_{Ru-ph-Ru} > \lambda_{Ru}$ with the exctintion coefficients in the order $\epsilon_{Ru-Ru} \approx 2\epsilon_{Ru} < \epsilon_{Ru-ph-Ru}$. The change in the band maximum is in accord with the predicted involvement of the BL for the lowest-lying MLCT transition in the dinuclear complexes and can be understood in terms of delocalization effects, see below.

From extensive investigations carried out by many research groups, it is known that light absorption by complexes of the Ru−polypyridine family ultimately results in population of lowest-lying, formally ^{3}MLCT, excited states with an efficiency of intersystem crossing assumed to be unity.[7a−c,26] The luminescence data listed in Table 1 indicate that **Ru-Ru** is remarkably more luminescent than the other complexes, the luminescence quantum yield being ∼150 times higher than that of **Ru** while an even larger increase of the lifetime is registered. As discussed below, this result is related to the different energy content of the luminescent excited states of **Ru-Ru**, **Ru-ph-Ru,** and **Ru** which exhibit room-temperature luminescence band maxima $\lambda_{max} = 720$, 656, and 640 nm, respectively, Table 1. Regarding the data obtained in frozen solvent (90 K, Table 1), only small differences in the lifetime values between the dinuclear and mononuclear complexes are observed.

Analysis of Luminescence Profiles. For the dinuclear complexes investigated, the MLCT excited state responsible for the luminescence involves the bridging ligands tpy-tpy and tpy-ph-tpy for **Ru-Ru** and **Ru-ph-Ru,** respectively. According to the approach developed by Meyer and co-workers,[20] it is possible to draw useful hints about the ability of a bridging ligand to allow delocalization of the promoted electron for such a MLCT (M → BL CT) excited state. The approach relates the extent of delocalization to the displacement of the potential-energy curve for the luminescent MLCT excited state with respect to the curve for the ground state (GS), i.e., a high degree of delocalization is accompanied by a small displacement. As shown by previous work,[20,32] analysis of the luminescence profiles affords the displacement parameter S_M along an accepting frequency, in our case C−C or C−N vibrations, $\hbar\omega_M = 1300-1400$ cm^{-1}, corresponding to the vibrational progression exhibited by the low-temperature luminescence spectra; Figure 2 shows an illustrative example. Table 2 compares results obtained from the analysis of the luminescence profiles of the dinuclear complexes, **Ru-Ru** and **Ru-ph-Ru,** and of the mononuclear complexes **Ru** and $Ru(bpy)_3^{2+}$.

Effect of Temperature on Luminescence. For the dinuclear complexes, we have measured the Ru-based luminescence lifetimes and spectra in the temperature interval from 300 to 90 K (frozen solvent). In all cases, the decay occurred as a single exponential. In Figure 3, the reciprocal of the lifetime, $1/\tau$, is plotted against the reciprocal of temperature, $1000/T$. As shown by many investigations dealing with the photophysics

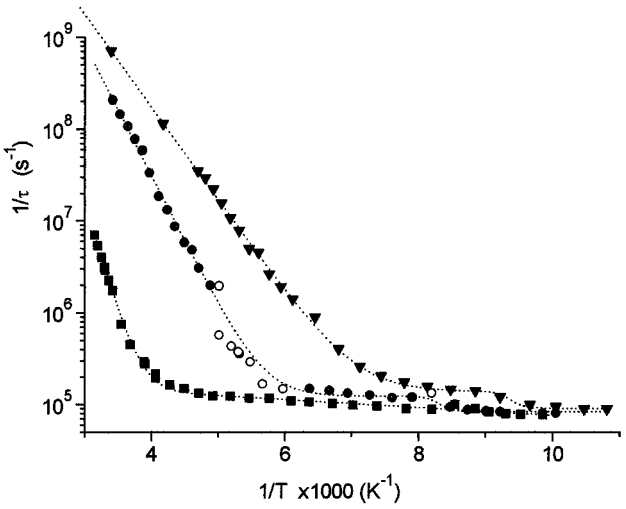

Figure 3. Plot of $1/\tau$ vs $1000/T$ for **Ru-Ru** (■), **Ru-ph-Ru** (●), and **Ru** (▼). Curve fit according to eqs 3a−c of text. Data for **Ru-ph-Ru** from 165 to 200 K (⊙) was excluded from the fit, see text.

TABLE 3: Kinetic Parameters for Excited-State Decay[a]

	A_1 (s^{-1})	ΔE_1 (cm^{-1})	$k_o + B$ (s^{-1})
Ru-Ru	1.7×10^{14}	3800	1.1×10^4 [b]
Ru-ph-Ru	1.5×10^{13}	2300	1.2×10^5 [c]
Ru	1.9×10^{12}	1600	1.4×10^5 [d]

[a] From least-squares nonlinear fitting of eqs 3a−c of the text to the experimental points of Figure 3. [b] $B = 0$; use of an additional Arrhenius term, eq 3b, gave $A_2 = 2 \times 10^5$ s^{-1} and $\Delta E_2 = 80$ cm^{-1}. [c] $B = 4 \times 10^4$ s^{-1}. [d] $B = 4.8 \times 10^4$ s^{-1}.

of Ru−polypyridine complexes, it is possible to analyze the temperature dependence of the luminescence lifetime according to an Arrhenius-type approach.[7a−c,32c,33,34] We employ the following simplified equations[7b,34] containing one or two Arrhenius-type terms, eqs 3a−c.

$$1/\tau = A_1 \exp\left(-\frac{\Delta E_1}{RT}\right) + k_o' \qquad (3a)$$

$$1/\tau = A_1 \exp\left(-\frac{\Delta E_1}{RT}\right) + A_2 \exp\left(-\frac{\Delta E_2}{RT}\right) + k_o' \qquad (3b)$$

$$k_o' = k_o + \frac{B}{1 + \exp[C(1/T - 1/T_B)]} \qquad (3c)$$

In the above equations, A_1 and ΔE_1 are the preexponential factor and the energy barrier, respectively, for thermal population of a higher-lying metal-centered (MC) state of dd orbital origin which is involved in the deactivation of the luminescent MLCT state. A_2 and ΔE_2 are parameters concerned with the fact that the luminescent level is actually composed by a cluster of MLCT excited states, and ΔE_2 can be viewed as the energy width of the clusterized levels. k_o' is a term which includes a low-temperature limiting rate constant, k_o (for the usual radiative and noradiative contributions at 90 K), and it may include a contribution, B, which takes care of effects occurring around the temperature T_B and concerned with the glass-to-fluid transition of the solvent.[7b,34] Within this empirical description, B is the increase of the nonradiative rate observed on passing from frozen to fluid solvent. In the present cases, T_B occurred in the interval 110−125 K, Figure 3, and B was in the range $4-5 \times 10^4$ s^{-1}.

Table 3 lists the A_1 and ΔE_1 parameters for the complexes studied. These parameters were evaluated by fitting the $1/\tau$ vs $1/T$ experimental points to eq 3a for **Ru-ph-Ru** and **Ru**,[13c] and eq 3b was required for the case of **Ru-Ru**. For the latter complex, the B term proved of no use because the $1/\tau$ vs $1/T$ experimental points did not exhibit the stepwise behavior related to the glass-to-fluid transition of the solvent, see Figure 3, and A_2 and ΔE_2 were 2×10^5 s^{-1} and 80 cm^{-1}, respectively. For **Ru-ph-Ru**, the emission decay between 165 and 200 K was poorly described by a single-exponential law, which we attributed to some aggregation. For this complex, experimental points from this temperature interval were excluded from the fit (Figure 3).

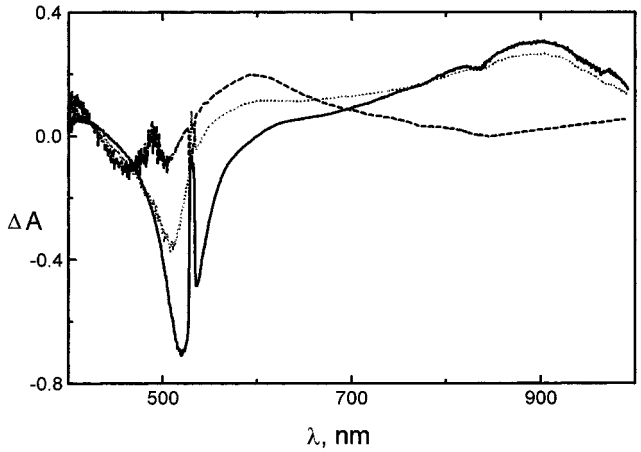

Figure 4. Transient absorption spectra of **Ru-Ru** (—), **Ru-ph-Ru** (•••), and **Ru** (- - -), as taken at the end of a 35 ps pulse ($\lambda_{exc} = 532$ nm, pulse energy ~3 mJ). Absorbances at 532 nm were adjusted for obtaining comparable intensities of the spectra on the band maxima.

Transient-Absorption Spectroscopy. Room-temperature absorption spectra detected at the end of a 35 ps laser pulse in acetonitrile solutions of **Ru-Ru**, **Ru-ph-Ru**, and **Ru** are shown in Figure 4. In the low-energy portion, the spectra for the dinuclear complexes are characterized by a broad band, maximizing at 900 nm; in this wavelength region, no maximum is present in the spectrum of **Ru**. The decay of the excited-state spectrum for **Ru** and **Ru-Ru** could be fit according to a a single-exponential decay, with lifetimes of 0.8 and 580 ns, respectively, in good agreement with the emission data, see Table 1. The decay of the spectrum of **Ru-ph-Ru** was not detected with sufficient precision because it occurred within a time window not covered by our instrumentation. This happened because it was too short for the nanosecond flash-photolysis equipment (resolution >10 ns) and too long for the picosecond system, where the delay line allows detection of spectra only within 3.3 ns. Nevertheless, the decay of the transient absorbance for **Ru-ph-Ru** was consistent with $\tau = 4$ ns, as obtained from the luminescence experiments.

Discussion

Delocalization of the Excited State. For the dinuclear complexes **Ru-Ru** and **Ru-ph-Ru**, the electrochemical data show that the bridging ligand is easier to reduce than the peripheral ttp ligand, i.e., the LUMO is centered on the bridging ligand and not on ttp. On this basis, the lowest-lying MLCT excited state is expected to be metal-to-bridging ligand in nature M → BL CT. For these levels, the electrochemical behavior of the compounds suggests an energy ordering $E_{\mathbf{Ru-Ru}} < E_{\mathbf{Ru-ph-Ru}} < E_{\mathbf{Ru}}$. On the basis of the effect of the size of the ligand, a decrease in the energy of the LUMO might be expected for the larger tpy-ph-tpy ligand with respect to the tpy-tpy ligand. However, the introduction of a phenylene spacer between the tpy units leads to a decrease of the delocalization of the π^* orbitals, due to a non-coplanar geometric arrangement of the

terpyridine moieties and of the inserted phenylene unit.[35] In spite of that, the phenylene spacers do not prevent the intersite communication, even for distances up to 20 Å.[13,22,31a] The spectroscopic properties examined in detail below enable the full understanding of the delocalization properties in the systems studied.

Ground-State Absorption Properties. For CT transitions, it can be shown that the energy position corresponding to the absorption maximum ($\tilde{\nu}_{abs}$, in cm^{-1}) and the intensity (ϵ) of the CT band are related to the extent of delocalization of the promoted electron from the donor to the acceptor site.[36] An approximate value for the transition dipole moment, $\vec{\mu}$, for the GS → ^{1}MLCT transition occurring in the complexes examined can be derived from the spectroscopic quantities obtained, eq 4, where f is the oscillator strength.

$$f \cong 4.3 \times 10^{-9} \int \epsilon d\tilde{\nu} \tag{4a}$$

$$|\vec{\mu}| = \left(\frac{f}{1.085 \times 10^{-5} \tilde{\nu}_{abs}} \right)^{1/2} \tag{4b}$$

According to current theories for CT transitions and within a simplified interaction scheme, $\vec{\mu}$ is mainly due to a "transfer term",[36b] eq 5, where β and E are the resonance integral and the separation energy, respectively, for the zero-order energy levels of the ground and excited states, e is the electronic charge and $\boldsymbol{R}_{ML}$ is the transition dipole length. Calculations according

$$\vec{\mu} = -\frac{\beta \boldsymbol{R}_{ML} e}{E} \tag{5}$$

to eqs 4 and 5 afford $\boldsymbol{R}_{ML}$, i.e., the distance covered by the electron promoted from the metal center over the ligand system.[37] Within this approach, a large value for $\boldsymbol{R}_{ML}$ would indicate an effective delocalizing ability of the ligand involved. From our spectroscopic data, we obtained $|\vec{\mu}| = 1.76$, 1.83, and 1.13 e Å for **Ru-Ru**, **Ru-ph-Ru**, and **Ru**, respectively. Thus, on the basis of the fact that in the dinuclear species there are two chromophoric groups and according to a rough approximation based on the use of the same β and E values, our absorption results suggest that the transition leading to population of the ^{1}MLCT excited state involves similar ligand fragments for the three cases. Notice that for the dinuclear complexes with respect to **Ru**, delocalization may be expected to decrease the LUMO orbital coefficients at the chelating positions of the bridging ligand (i.e., the one responsible for the lowest-energy absorption band). This would result in a decrease of the orbital overlap between the metal-centered and ligand-centered orbitals and, in turn, to a decrease of β. Therefore, for the dinuclear complexes with respect to **Ru**, the value of β could be significantly smaller, thus masking a possible increase of $\boldsymbol{R}_{ML}$, see eq 5. In conclusion, the size of the accepting ligand appears to be related to changes in the energy position of the band maximum while absorption intensities are not significantly affected, which may be due to opposite variations of β and $\boldsymbol{R}_{ML}$ parameters.

Excited-State Absorption Properties. The triplet spectra for the **Ru-Ru**, **Ru-ph-Ru**, and **Ru** complexes are characterized by similar features in the UV region, attributable to LC absorption properties, and in the region around 500 nm, where bleaching of the ground-state MLCT absorption bands is observed.[10,12,17,38] Above 550 nm, the spectra are characterized by broad bands which maximize around 600 and 900 nm for **Ru** and the dinuclear species, respectively, Figure 4. Prior work by Amouyal and colleagues[38] dealing with some mononuclear Ru−terpy complexes has shown that their transient spectra and the spectra of the reduced, uncomplexed ligands were similar, exhibiting band maxima around 600 nm.[38] On the basis of this result and owing to the MLCT nature of the excited state, we ascribe the spectral behavior of our complexes above 550 nm to intraligand transitions of the corresponding ligand radical anions. Thus, the hypochromic shift of the band maximum for **Ru-Ru** and **Ru-ph-Ru** with respect to **Ru** may result from the fact that the π^* orbitals are more closely spaced in terms of energy. This explanation, though stated in somewhat qualitative terms because it does not rely on an analysis of allowed or forbidden transitions,[39] may account for the observed spectral behavior, Figure 4. A hypochromic shift of the band maximum on passing from the mononuclear to the dinuclear complexes was already observed in complexes of ruthenium(II) incorporating polyene,[17a] ethenyl,[17b,21] or ethynyl[12] groups within the bridging ligand and was likewise ascribed to delocalization effects for intraligand transitions.

TABLE 4: Radiative and Nonradiative Rate Constants for Room-Temperature Decay of MLCT Excited State

	k_r[a] (s^{-1})	k_{nr}[a] (s^{-1})	k_{nr}^{act}[b] (s^{-1})	k_{nr}^{dir}[c] (s^{-1})
Ru-Ru[c]	8.2×10^3	1.8×10^6	1.3×10^6	8.3×10^4
Ru-ph-Ru[b]	2.8×10^4	2.5×10^8	1.9×10^8	1.0×10^5
Ru[b]	3.6×10^4	1.1×10^9	7.3×10^8	1.1×10^5

[a] Based on eqs 6 of the text. [b] Based on $k_{nr}^{act} = A_1 \exp(-\Delta E_1/RT)$, eq 3a of the text. [c] As estimated from data taken at 130 K: $k_{nr}^{dir} = \tau^{-1}(130\ K) - k_r - k_{nr}^{act}(130\ K)$.

Radiative and Nonradiative Processes for Deactivation of the Luminescence. From the room-temperature luminescence lifetimes and quantum yields of Table 1, it is possible to obtain the rate constants for the radiative (k_r) and nonradiative (k_{nr}) processes, eq 6, which contribute to deactivation of the MLCT luminescent excited states.

$$k_r = \Phi/\tau \tag{6a}$$

$$k_{nr} = (1 - \Phi)/\tau \tag{6b}$$

Values for the k_r and k_{nr} rate constants are collected in Table 4. These data show that (i) k_r is larger for higher-lying excited states, consistent with the known relation[40] that $k_r \propto \tilde{\nu}_{em}^3$ (with the emission maximum $\tilde{\nu}_{em}$ in cm^{-1}) and that (ii) the luminescence lifetime at room temperature is governed by nonradiative transitions, $\tau^{-1} \sim k_{nr}$.[7a−c] Now we will discuss the relative importance of the paths which contribute to the nonradiative decay of the luminescent level.

According to a detailed approach developed in the 1970s and onward,[41] one has to consider (i) nonradiative transitions directly connecting the ^{3}MLCT luminescent level (or the cluster of close-lying luminescent levels) and the ground state and (ii) transitions occurring via thermal population of higher-lying ^{3}MC levels. Figure 5 provides a frequently employed pictorial description for the potential-energy curves of the GS and the MLCT, and MC states involved.[7a−c] Within this illustration, the MLCT potential-energy curve is only slightly displaced with respect to that for the GS. On the contrary, the MC curve is strongly displaced and the ensuing MC−GS strong coupling results in fast radiationless transitions. These can lead to a return to ground state but may also include photochemical processes depending on the solvent and counterion.[41h,i,42] Note that the relevant vibrational modes coupling each pair of states is not necessarily the same, but a single x-axis is sufficient for this simplified representation.

The available approaches for disentangling the two types of contributions are based on (i) the analysis of the luminescence

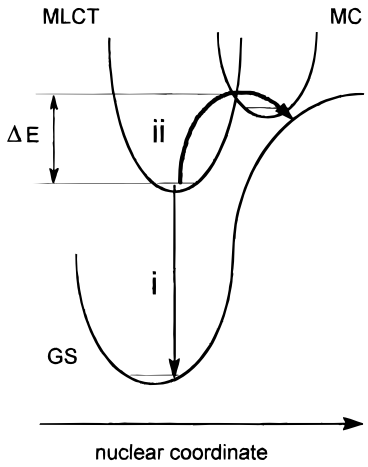

Figure 5. Two nonradiative paths for deactivation of the luminescent MLCT excited state: (i) direct MLCT−GS transition, and (ii) thermally activated, irreversible population of a MC state and return to GS. The radiative MLCT−GS transition is not shown.

profiles as performed on data obtained at low temperature,[20] where the activated path is unimportant,[43] and (ii) the study of the temperature dependence of the luminescence lifetime,[7a−c,33,34,41] see below.

(i) Excited-State Decay Direct to Ground State. The results of the emission spectral fits for the luminescence profiles obtained at 90 K are reported in Table 2. The values for the displacement parameter S_M, the electron-vibrational coupling constant along the (average frequency) C−C and C−N vibrations of the accepting ligand (i.e., BL), are 0.35, 0.46, and 0.53 for **Ru-Ru**, **Ru-ph-Ru**, and **Ru**, respectively. With reference to Figure 5, this indicates that in the series of examined complexes the energy curve for the luminescent state of **Ru-Ru** is the least displaced with respect to that for the ground state. As thorougly discussed by Meyer and co-workers for the MLCT luminescent state of complexes of the Ru(II)−, Os(II)−, and Re(I)−polypyridine families,[20] a low value for S_M is related to an efficient electron delocalization over the accepting ligand system, which results in smaller structural changes along the C−C and C−N bonds. In our cases, this effect is likely associated with the large and rigid bridging ligands employed, as also suggested by comparison with the case of $Ru(bpy)_3^{2+}$, Table 2, where the smaller bpy ligand is expected to undergo larger structural rearrangements and $S_M = 0.87$. Notice that this effect is also related to the energy separation between the MLCT and ground levels, due to the observation that for smaller and smaller separations, back-bonding effects (which imply extended delocalization) are maximized.[20]

(ii) Activated Decay via MC States. The kinetic parameters for the excited-state decay of the complexes examined, Table 3, show that (a) the photophysical behavior is expected to be strongly affected by temperature and (b) in the high-temperature region, i.e., at room temperature, deactivation of the MLCT excited state is governed by a kinetically similar deactivation process. According to previous treatments,[7a−c,33,34,41] this implies population of a higher-lying MC state which is in turn so strongly coupled to the ground state that the rate constant for the MC → GS step is much higher than that for the backward MC → MLCT step. This represents a limiting kinetic case whereby the prexeponential factor of eqs 3a−c, A_1, is in the range $10^{12}-10^{14}$ s^{-1} and ΔE_1 is the energy difference between the bottom of the luminescent MLCT curve and the crossing point between the MLCT and MC curves, see Figure 5. Thus, according to the illustration depicted in this figure, the excited-state delocalization results both in vertical and horizontal shifts for the MLCT energy curve, consistent with the observed changes in emission energy and ΔE_1. Note that similar ligand-field strengths are to be expected for the three cases, owing to the identical tridentate sites of the tpy-tpy, tpy-ph-tpy, and ttp ligands. Therefore, the MC levels for the complexes investigated are expected to lie at approximately constant energy values.

Relative Importance of Direct and Activated Nonradiative Paths. It is interesting to compare the room temperature relative contributions of radiationless processes to the excited state decay, steps i and ii in Figure 5. As for path i, an estimate of the rate constant may be obtained from the data at 130 K, i.e., (a) above the glass-to-fluid transition region and where (b) only minor contributions from the activated path must be taken into account, see Figure 3. Evaluated values are collected in Table 4, based on $k_{nr}^{dir} = \tau^{-1}(130\ K) - k_r - k_{nr}^{act}(130\ K)$. Thus, $k_{nr}^{dir} = 8.3 \times 10^4$, 1.0×10^5, and 1.1×10^5 s^{-1} for **Ru-Ru**, **Ru-ph-Ru**, and **Ru**, respectively. The room-temperature activated path ii of Figure 5 occurs with rate constants $k_{nr}^{act} = 1.3 \times 10^6$, 1.9×10^8, and 7.3×10^8 s^{-1} for **Ru-Ru**, **Ru-ph-Ru**, and **Ru**, respectively, as calculated from $k_{nr}^{act} = A_1 \exp(-\Delta E_1/RT)$, Table 4. Thus, the ratio $k_{nr}^{act}/k_{nr}^{dir} \approx 16$, 1900, and 7000 for **Ru-Ru**, **Ru-ph-Ru**, and **Ru**, respectively. From these figures, one sees that at room temperature thermal access of the MC state represents in each case the predominant decay path for the luminescent MLCT level while contributions related to the energy-gap law[19] seem to play a modest role.

Notice that according to the energy-gap law, one expects the linear relation of eq 7 to hold,[19,20] where $E_o = E_{00} + S_L\hbar\omega_L$ and $\gamma = \ln[E_o/(S_M\hbar\omega_M)] - 1$.[20] On the basis of the data from

$$\ln(k_{nr}^{dir}) \propto -S_M - \gamma\frac{E_o}{\hbar\omega_M} \qquad (7)$$

Table 2, a substantial increase in k_{nr}^{dir} is expected on passing from **Ru** to **Ru-Ru**. However, the obtained values for k_{nr}^{dir} (as estimated for 130 K, see above) do not conform to predictions based on eq 7. Instead, k_{nr}^{dir} is found to be slightly larger for **Ru** than for **Ru-Ru**. Of course, this conclusion relies on a limited set of compounds and should, therefore, be taken with some caution.

Consequences of Delocalization for the Development of Photosensitizers. As pointed out previously, particularly by Meyer and co-workers,[18,44] delocalization of the MLCT state is useful for the construction of Ru(II) sensitizers that absorb in the red region of the visible spectrum and still avoid the rapid nonradiative deactivation (k_{nr}^{dir}) predicted by the energy-gap law. However, for the present (restricted) series of tpy-based complexes, by far the most significant effect of delocalization (at room temperature) is the decrease of the deactivation via MC states (k_{nr}^{act}). An interesting outcome is that the photophysical properties of **Ru-Ru** satisfactorily match those of $Ru(bpy)_3^{2+}$ [7a−c] while retaining the favorable structural properties of the bis(tpy) Ru(II) complexes.[10] This makes **Ru-Ru** a useful building block to be incorporated as a central core into rigid, linearly arranged multicomponent systems.[10,12,13,29] For instance, the study of interesting multistep electron transfer and charge separation processes would likely be possible if additional electroactive (and photoactive) electron-donating (D) and -accepting (A) units will be located on the main symmetry axis, Chart 3.

Conclusions

We have investigated the role of electron delocalization on the photophysics of the dinuclear complexes of ruthenium(II)

CHART 3

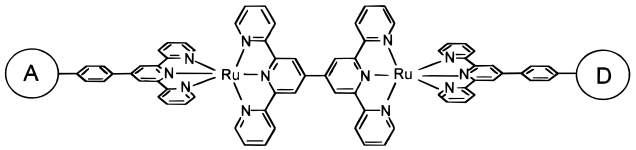

shown in Chart 2. In these compounds, the rigid bridging ligands contain tpy chelating sites separated by ph_n spacers ($n = 0-1$, the intermetal distance varies from 11 to 15.5 Å)[10c,22] and the terminal ligand is ttp. The luminescent level of the dinuclear complexes has a metal-to-bridging ligand electronic configuration, and from the observed luminescence properties, both at room temperature and at 90 K, from the temperature dependence of the luminescence lifetime, and from the shape of the transient absorption spectra, we have characterized the decay processes of the excited states. The **Ru-Ru** complex exhibits a stronger and longer-lived luminescence ($\Phi = 4.7 \times 10^{-3}$ and $\tau = 570$ ns) than either the **Ru-ph-Ru** dinuclear species ($\Phi = 1.1 \times 10^{-4}$ and $\tau = 4$ ns) or the parent **Ru** mononuclear complex ($\Phi = 3.2 \times 10^{-5}$ and $\tau = 0.9$ ns). For the complexes examined, we have shown that decay of the luminescent level occurs predominantly via thermal access of upper-lying MC states. Because of electron delocalization, for **Ru-Ru** this path is less efficient, leading to a room-temperature nonradiative rate constant which is smaller by ca. two orders of magnitude than that of **Ru-ph-Ru** or **Ru**.

Acknowledgment. This work was supported by the Progetto Strategico Tecnologie Chimiche Innovative of CNR, Italy. F.B. thanks Prof. Thomas J. Meyer for kindly providing the software for the vibronic analysis of the profiles of the luminescence spectra. L.H. acknowledges personal grants from The European Commission (TMR Contract No. ERBFMBICT950352) and The Foundation Blanzeflor Ludovisi-Boncompagni, née Bildt. We thank M. Minghetti and L. Ventura for technical assistance.

References and Notes

(1) (a) *Tetrahedron* **1989**, *45* (Special Issue). (b) *Photoinduced Electron Transfer*; Fox, M. A., Chanon, M., Eds.; Elsevier: New York, 1988; Parts A−D. (c) *Top. Curr. Chem.* **1990**, *156*; **1990**, *158*; **1991**, *159*. (d) *Supramolecular Chemistry*; Balzani, V., De Cola, L., Eds.: Kluwer: Dortrecht, The Netherlands, 1992. (e) Jordan, K.; Paddon-Row, M. N. *Chem. Rev.* **1992**, *92*, 395 and references therein. (f) *New J. Chem.* **1996**, *20* (Special Issue), 723−915.

(2) (a) Marcus, R. A.; Sutin, N. *Biochim. Biophys. Acta* **1985**, *811*, 265. (b) Marcus, R. A. *Angew. Chem., Int. Ed. Engl.* **1993**, *32*, 1111. (c) Closs, G. L.; Miller, J. R. *Science* **1988**, *240*, 440. (d) Closs, G. L.; Johnson, M. D.; Miller, J. R.; Piotrowiak, P. *J. Am. Chem. Soc.* **1989**, *111*, 3751.

(3) (a) Kurrek, H.; Huber, M. *Angew. Chem., Int. Ed. Engl.* **1995**, *34*, 849. (b) Gust, D.; Moore, T. *Top. Curr. Chem.* **1991**, *159*, 103. (c) Wasielewski, M. R. *Chem. Rev.* **1992**, *92*, 365.

(4) Molnar, S. M.; Nallas, G.; Bridgewater, J. S.; Brewer, K. J. *J. Am. Chem. Soc.* **1994**, *116*, 5206.

(5) (a) Webber, S. E. *Chem. Rev.* **1990**, *90*, 1469. (b) Denti, G.; Campagna, S.; Serroni, S.; Ciano, M.; Balzani, V. *J. Am. Chem. Soc.* **1992**, *114*, 2944. (c) Stewart, G.; Fox, M. A. *J. Am. Chem. Soc.* **1996**, *118*, 4354. (d) Devadoss, C.; Bharati, P.; Moore, J. S. *J. Am. Chem. Soc.* **1996**, *118*, 9635.

(6) (a) Balzani, V.; Scandola, F. In *Comprehensive Supramolecular Chemistry*; Reinhout, D. N., Ed.; Pergamon: Oxford, 1996; Vol. 10, p 1. (b) Debreczeny, M. P.; Svec, W. A.; Wasielewski, M. R. *Science* **1996**, *274*, 584. (c) Ballardini, R.; Balzani, V.; Credi, A.; Gandolfi, M. T.; Langford, S. J.; Menzer, S.; Prodi, L.; Stoddart, J. F.; Venturi, M.; Williams, D. J. *Angew. Chem., Int. Ed. Engl.* **1996**, *35*, 978. Some recent examples employing Ru(II)-based components are reported, see: (d) Haga, M.-a.; Ali, Md. M.; Arakawa, R. *Angew. Chem., Int. Ed. Engl.* **1996**, *35*, 76. (e) Szemes, F.; Hesek, D.; Chen, Z.; Dent, S. W.; Drew, M. G. B.; Goulden, A. J.; Graydon, A. R.; Grieve, A.; Mortimer, R. J.; Wear, T.; Weightman, J. S.; Beer, P. D. *Inorg. Chem.* **1996**, *35*, 5868. (f) Kropf, M.; Joselevich, E.; Dürr, H.; Willner, I. *J. Am. Chem. Soc.* **1996**, *118*, 655. (g) Beer, P. D.; Dent, S. W.; Hobbs, G. S.; Wear, T. J. *Chem. Commun.* **1997**, 99.

(7) (a) Meyer, T. J. *Pure Appl. Chem.* **1986**, *58*, 1193. (b) Juris, A.; Balzani, V.; Barigelletti, F.; Campagna, S.; Belser, P.; von Zelewsky, A. *Coord. Chem. Rev.* **1988**, *84*, 85. (c) Meyer, T. J. *Acc. Chem. Res.* **1989**, *22*, 163. (d) Kalyanasundaram, K. *Photochemistry of Polypyridine and Porphyrine Complexes*; Academic Press: London, 1991. (e) *Photosensitization and Photocatalysis Using Inorganic and Organometallic Compounds*; Kalyanasundaram, K., Grätzel, M., Eds.; Kluwer: Dortrecht, The Netherlands, 1993. (f) Schanze, K. S.; MacQeen, D. B.; Perkins, T. A.; Cabana, L. A. *Coord. Chem. Rev.* **1993**, *122*, 63. (g) Didier, P.; Ortmans, I.; Kirsch-De Mesmaeker, A.; Watts, R. *Inorg. Chem.* **1993**, *32*, 5239. (h) Nallas, G. N. A.; Jones, S. W.; Brewer, K. J. *Inorg. Chem.* **1996**, *35*, 6974. (i) Bignozzi, C. A.; Schoonover, J. N.; Scandola, F. *Prog. Inorg. Chem.* **1997**, *44*, 1.

(8) (a) Balzani, V.; Juris, A.; Venturi, M.; Campagna, S.; Serroni, S. *Chem. Rev.* **1996**, *96*, 759. (b) Scandola, F.; Indelli, M. T.; Chiorboli, C.; Bignozzi, C. A. *Top. Curr. Chem.* **1990**, *158*, 63. For a few recent examples of multicomponent systems incorporating photoactive complexes, see: (c) Ho, P. K.-K.; Cheung, K.-K.; Che, C.-M. *Chem. Commun.* **1996**, 1197. (d) Vogler, L. M.; Brewer, K. J. *Inorg. Chem.* **1996**, *35*, 818. (e) Bolger, J.; Gordon, A.; Ishow, E.; Launay, J.-P. *J. Chem. Soc., Chem. Commun.* **1995**, 1799. (f) Wärnmark, K.; Thomas, J. A.; Heyke, O.; Lehn, J.-M. *Chem. Commun.* **1996**, 701.

(9) (a) Von Zelewsky, A. *Stereochemistry of Coordination Compounds*; Wiley: Chichester, 1996. (b) Rutherford, T. J.; Reitsma, D. A.; Keene, F. R. *J. Chem. Soc., Dalton Trans.* **1994**, 3659.

(10) (a) Harriman, A.; Ziessel, R. *Chem. Commun.* **1996**, 1707. (b) Constable, E. C.; Cargill Thompson A. M. W. *New J. Chem.* **1996**, *20*, 65. (c) Sauvage, J.-P.; Collin, J.-P.; Chambron, J.-C.; Guillerez, S.; Coudret, C.; Balzani, V.; Barigelletti, F.; De Cola, L.; Flamigni, L. *Chem. Rev.* **1994**, *94*, 993. (b) Armspach, D.; Constable, E. C.; Housecroft, C. E.; Neuburger, M.; Zehnder, M. *New J. Chem.* **1996**, *20*, 331.

(11) Maestri, M.; Armaroli, N.; Balzani, V.; Constable, E. C.; Cargill Thompson, A. M. W. *Inorg. Chem.* **1995**, *34*, 2759.

(12) (a) Benniston, A. C.; Grosshenny, V.; Harriman, A.; Ziessel, R. *Angew. Chem., Int. Ed. Engl.* **1994**, *33*, 1884. (b) Grosshenny, V.; Harriman, A.; Ziessel, R. *Angew. Chem., Int. Ed. Engl.* **1995**, *34*, 1100. (c) Grosshenny, V.; Harriman, A.; Ziessel, R. *Angew. Chem., Int. Ed. Engl.* **1995**, *34*, 2705. (d) Grosshenny, V.; Harriman, A.; Hissler, M.; Ziessel, R. *J. Chem. Soc., Faraday Trans.* **1996**, *92*, 2223.

(13) (a) Barigelletti, F.; Flamigni, L.; Collin, J.-P.; Sauvage, J.-P. *Chem. Commun.* **1997**, 333. (b) Barigelletti, F.; Flamigni, L.; Balzani, V.; Sauvage, J.-P.; Collin, J.-P.; Sour, A.; Constable, E. C.; Cargill Thompson, A. M. W. *J. Am. Chem. Soc.* **1994**, *116*, 7692. (c) Hammarström, L.; Barigelletti, F.; Flamigni, L.; Armaroli, N.; Sour, A.; Sauvage, J.-P.; Collin, J.-P. *J. Am. Chem. Soc.* **1996**, *118*, 7692. (d) Indelli, M. T.; Scandola, F.; Collin, J.-P.; Sauvage, J.-P.; Sour, A. *Inorg. Chem.* **1996**, *35*, 303.

(14) (a) Willner, I.; Willner, B. *Top. Curr. Chem.* **1991**, *159*, 153. (b) Fox, M. A.; Jones, W. E., Jr.; Watkins, D. M. *Chem. Eng. News* **1993**, *71*, 38. (c) Bard, A. J.; Fox, M. A. *Acc. Chem. Res.* **1995**, *28*, 8. 141.

(15) (a) Winkler, J. R.; Netzel, T. L.; Creutz, C.; Sutin, N *J. Am. Chem. Soc.* **1987**, *109*, 2381. (b) Stone, M. L.; Crosby, G. A. *Chem. Phys. Lett.* **1981**, *79*, 169.

(16) Barigelletti, F.; Flamigni, L.; Guardigli, M.; Sauvage, J.-P.; Collin, J.-P.; Sour, A. *Chem. Commun.* **1996**, 1329.

(17) (a) Benniston, A. C.; Goulle, V.; Harriman, A.; Lehn, J.-M.; Marczinke, B. *J. Phys. Chem.* **1994**, *98*, 7798. (b) Grosseny, V.; Harriman, A.; Romero, F. R.; Ziessel, R. *J. Phys. Chem.* **1996**, *100*, 17472.

(18) (a) Treadway, J. A.; Loeb, B.; Lopez, R.; Anderson, P. A.; Keene, F. R.; Meyer, T. J. *Inorg. Chem.* **1996**, *35*, 2242. (b) Strouse, G. F.; Schoonover, J. R.; Duesing, R.; Boyde, S.; Jones, W. E.; Meyer, T. J. *Inorg. Chem.* **1995**, *34*, 473.

(19) (a) Caspar, J. V.; Kober, E. M.; Sullivan, B. P.; Meyer, T. J. *J. Am. Chem. Soc.* **1982**, *104*, 630. (b) Englman, R.; Jortner, J. *Mol. Phys.* **1970**, *18*, 145. (c) Freed, K.; Jortner, J. *J. Chem. Phys.* **1970**, *52*, 6272.

(20) (a) Caspar, J. V.; Meyer, T. J. *Inorg. Chem.* **1983**, *22*, 2444. (b) Caspar, J. V.; Meyer, T. J. *J. Am. Chem. Soc.* **1983**, *105*, 5583. (c) Allen, G. H.; White, R. P.; Rillema, D. P.; Meyer T. J. *J. Am. Chem. Soc.* **1984**, *106*, 2613. (d) Caspar, J. V.; Westmoreland, T. D.; Allen, G. H.; Bradley, P. G.; Meyer, T. J.; Woodruff, W. H. *J. Am. Chem. Soc.* **1984**, *106*, 3492. (e) Kober, E. M.; Caspar, J. V.; Lumpkin, R. S.; Meyer T. J. *J. Phys. Chem.* **1986**, *90*, 3722. (f) Barqawi, K. R.; Murtaza, Z.; Meyer, T. J. *J. Phys. Chem.* **1991**, *95*, 47. (g) Worl, L. A.; Duesing, R.; Chen, P.; Della Ciana, L.; Meyer, T. J. *J. Chem. Soc., Dalton. Trans.* **1991**, 849. (h) Claude, J. P.; Meyer, T. J. *J. Phys. Chem.* **1995**, *99*, 51.

(21) Baba, H. I.; Ensley, H. E.; Schmehl, R. H. *Inorg. Chem.* **1995**, *34*, 1198.

(22) Collin, J.-P.; Lainé, P.; Launay, J.-P.; Sauvage, J.-P.; Sour, A. *J. Chem. Soc., Chem. Commun.* **1993**, 434.

(23) Collin, J.-P.; Harriman, A.; Heitz, V.; Odobel, F.; Sauvage, J.-P. *J. Am. Chem. Soc.* **1994**, *116*, 5679.

(24) Demas, J. N.; Crosby, G. A. *J. Phys. Chem.* **1971**, *75*, 991.

(25) Nakamaru, K. *Bull. Chem. Soc. Jpn.* **1982**, *55*, 2697.

(26) (a) Demas, J. N.; Crosby, G. A. *J. Am. Chem. Soc.* **1971**, *93*, 2841. (b) Bensasson, R.; Salet, C.; Balzani, V. *J. Am. Chem. Soc.* **1976**, *98*, 3722. (c) Demas, J. N.; Crosby, G. A. *Inorg. Chem.* **1979**, *18*, 3177. (d) Bolletta, F.; Juris, A.; Maestri, M.; Sandrini, D. *Inorg. Chim. Acta* **1980**, *44*, L175.

(27) Beley, M.; Chodorowsky, S.; Collin. J.-P.; Sauvage, J.-P.; Flamigni, L.; Barigelletti, F. *Inorg. Chem.* **1994**, *33*, 2543.

(28) Bevington, P. R. T. *Data Reduction and Error Analysis for Physical Sciences*; McGraw-Hill: New York, 1969.

(29) Collin, J.-P.; Guillerez, S.; Sauvage, J.-P.; Barigelletti, F.; De Cola, L.; Flamigni, L.; Balzani, V. *Inorg. Chem.* **1991**, *30*, 4230.

(30) (a) Vlcek, A. A.; Dosdworth, E. S.; Pietro, W. J.; Lever, A. B. P. *Inorg. Chem.* **1995**, *34*, 1906 and references therein. (b) Barigelletti, F.; Juris, A.; Balzani, V.; Belser, P.; Von Zelewsky, A. *Inorg. Chem.* **1987**, *26*, 4115.

(31) Exceptions to this behavior are found when the bridging ligands bear negative charges so that the lowest-lying MLCT states are centered on the terminal ligands, see, for instance: (a) Barigelletti, F.; Flamigni, L.; Guardigli, M.; Juris, A.; Beley, M.; Chodorowski-Kimmes, S.; Collin, J.-P.; Sauvage, J.-P. *Inorg. Chem.* **1996**, *35*, 1360. (b) Barigelletti, F.; De Cola, L.; Balzani, V.; Hage, R.; Hasnoot, J. G.; Reedijk, J.; Vos, J. G. *Inorg. Chem.* **1991**, *30*, 641.

(32) (a) Baiano, J. A.; Kessler, R. J.; Lumpkin, R. S.; Munley, M. J.; Murphy, W. R., Jr. *J. Phys. Chem.* **1995**, *99*, 17680. (b) Liang, Y. Y.; Baba, A. I.; Kim, W. Y.; Atherton, S. J.; Schmehel, R. H. *J. Phys. Chem.* **1996**, *1001*, 18408. (c) Macatangay, A.; Zheng, G. Y.; Rillema, D. P.; Jackman, D. C.; Merkert, J. W. *Inorg. Chem.* **1996**, *35*, 6823.

(33) (a) Islam, A.; Ikeda, N.; Nozaki, K.; Ohno, T. *Chem. Phys. Lett.* **1996**, *263*, 209. (b) Wallace, L.; Jackman, D. C.; Rillema, D. P.; Merkert, J. W. *Inorg. Chem.* **1995**, *34*, 5210. (c) Hughes, H. P.; Vos, J. G. *Inorg. Chem.* **1995**, *34*, 4001. (d) Maruszewski, K.; Kincaid, J. R. *Inorg. Chem.* **1995**, *34*, 2002. (e) Maruszewski, K.; Bajdor, K.; Strommen, D. P.; Kincaid, J. R. *J. Phys. Chem.* **1995**, *99*, 6286. (f) Sykora, M.; Kincaid, J. R. *Inorg. Chem.* **1995**, *34*, 5852. (g) Wang, R.; Vos, J. G.; Schmehl, R. H.; Hage, R. *J. Am. Chem. Soc.* **1992**, *114*, 1964. (h) Barigelletti, F.; De Cola, L.; Juris, A. *Gazz. Chim. Ital.* **1990**, *120*, 545. (i) Lumpkin, R. S.; Kober, E. M.; Worl, L. A.; Murtaza, Z.; Meyer, T. J. *J. Phys. Chem.* **1990**, *94*, 239. (l) Ryu, C. K.; Schmehl, R. H *J. Phys. Chem.* **1989**, *93*, 7966. (m) Kawanishi, Y.; Kitamura, N.; Tazuke, S. *Inorg. Chem.* **1989**, *28*, 2968.

(34) (a) Barigelletti, F.; Juris, A.; Balzani, V.; Belser, P.; Von Zelewsky, A. *J. Phys. Chem.* **1987**, *91*, 1095. (b) Barigelletti, F.; Belser, P.; Von Zelewsky, A.; Juris, A.; Balzani, V. *J. Phys. Chem.* **1985**, *89*, 3680.

(35) (a) Kim, Y.; Lieber, C. *Inorg. Chem.* **1989**, *28*, 3990. (b) Helms, A.; Heiler, D.; McLendon, G. *J. Am. Chem. Soc.* **1991**, *113*, 4325; **1992**, *114*, 6227. (c) Osuka, A.; Nakajima, S.; Maruyama, K.; Mataga, N.; Asahi, T.; Yamazaki, I.; Nishimura, Y.; Ohno, T.; Nozaki, K. *J. Am. Chem. Soc.* **1993**, *115*, 4577.

(36) (a) Hush, N. *Prog. Inorg. Chem.* **1967**, *8*, 391. (b) Day, P.; Sanders, N. *J. Chem. Soc. A* **1967**, 1536. (c) Ceulemans, A.; Vanquickenborne, L. G. *J. Am. Chem. Soc.* **1981**, *103*, 2238. (d) Phifher, C. C.; McMillin, D. R. *Inorg. Chem.* **1986**, *25*, 1329. (e) Richardson, D. E.; Taube, H. *J. Am. Chem. Soc.* **1983**, *105*, 40.

(37) According to an LCAO approach, it is possible to correlate the atomic contribution to the LUMO orbital of the chelating positions to the transition dipole moment, see, for instance, ref 36d and (a) Chen, P.; Curry, M.; Meyer, T. J. *Inorg. Chem.* **1989**, *28*, 2271. (b) Mines, G. A.; Roberts, J. A.; Hupp, J. T. *Inorg. Chem.* **1992**, *31*, 125. (c) De Cola, L.; Barigelletti, F. *Inorg. Chim. Acta* **1989**, *159*, 169.

(38) Amouyal, E.; Mouallem-Bahout, M.; Calzaferri, G. *J. Phys. Chem.* **1991**, *95*, 7641.

(39) (a) Zahradník, R.; Chársky, P. *J. Phys. Chem.* **1970**, *74*, 1235; **1970**, *74*, 1240; **1970**, *74*, 1249.

(40) Birks, J. B. *Photophysics of Aromatic Molecules*; Wiley: London, 1970; Chapter 4.

(41) (a) Harrigan, R. W.; Crosby, G. A. *J. Chem. Phys.* **1973**, *59*, 3468. (b) Hager, G. D.; Crosby, G. A. *J. Am. Chem. Soc.* **1975**, *97*, 7031. (c) Hager, G. D.; Watts, R. J.; Crosby, G. A. *J. Am. Chem. Soc.* **1975**, *97*, 7037. (d) Hipps, K. W.; Crosby, G. A. *J. Am. Chem. Soc.* **1975**, *97*, 7042. (e) Crosby, G. A.; Elfring, W. H., Jr. *J. Phys. Chem.* **1976**, *80*, 2206. (f) Elfring, W. H., Jr.; Crosby, G. A. *J. Am. Chem. Soc.* **1981**, *103*, 2683. (g) Kemp, T. J. *Prog. React. Kinet.* **1980**, *10*, 301. (h) Van Houten, J.; Watts, R. J. *J. Am. Chem. Soc.* **1976**, *98*, 4853. (i) Durham, B.; Caspar, J. V.; Nagle, J. K.; Meyer, T. J. *J. Am. Chem. Soc.* **1982**, *104*, 4803. (j) Caspar, J. V.; Meyer, T. J. *J. Am. Chem. Soc.* **1983**, *105*, 5583. (k) Caspar, J. V.; Meyer, T. J. *Inorg. Chem.* **1983**, *22*, 2444. (l) Allen, G. H.; White, R. P.; Rillema, D. P.; Meyer, T. J. *J. Am. Chem. Soc.* **1984**, *106*, 2613.

(42) (a) Van Houten, J.; Watts, R. J. *Inorg. Chem.* **1978**, *17*, 3381. (b) Ross, H. B.; Boldaji, M.; Rillema, D. P.; Blanton, C. B.; White, R. P. *Inorg. Chem.* **1989**, *28*, 1013. (c) Rillema, D. P.; Blanton, C. B.; Shaver, R. J.; Jackman, D. C.; Boldaji, M.; Bundy, S.; Worl, L. A.; Meyer, T. J. *Inorg. Chem.* **1992**, *31*, 1600.

(43) The radiative rate constant is practically independent of temperature, and the direct nonradiative transition (k_{nr}^{dir}) is expected to exhibit a weak temperature dependence above 90 K, see ref 20h, except around the glass-to-fluid transition, refs 7a−c and 34.

(44) Anderson, P. A.; Strouse, G. F.; Treadway, J. A.; Keene, F. R.; Meyer, T. J. *Inorg. Chem.* **1994**, *33*, 3863.